ORIGINAL ARTICLE

JBMR®

Adynamic Bone Decreases Bone Toughness During Aging by Affecting Mineral and Matrix

Adeline H Ng,[1,2] Sidney Omelon,[3] Fabio Variola,[4,5] Bedilu Allo,[2] Thomas L Willett,[2,6] Benjamin A Alman,[7,8] and Marc D Grynpas[1,2]

[1]Department of Laboratory Medicine and Pathobiology, University of Toronto, Toronto, Canada
[2]Lunenfeld-Tanenbaum Research Institute, Mount Sinai Hospital, Toronto, Canada
[3]Department of Chemical and Biological Engineering, University of Ottawa, Ottawa, Canada
[4]Department of Mechanical Engineering, University of Ottawa, Ottawa, Canada
[5]Department of Physics, University of Ottawa, Ottawa, Canada
[6]Department of Surgery, University of Toronto, Toronto, Canada
[7]Program in Developmental and Stem Cell Biology, Hospital for Sick Children, Toronto, Canada
[8]Department of Orthopaedic Surgery, Duke University, Durham, NC, USA

ABSTRACT

Adynamic bone is the most frequent type of bone lesion in patients with chronic kidney disease; long-term use of antiresorptive therapy may also lead to the adynamic bone condition. The hallmark of adynamic bone is a loss of bone turnover, and a major clinical concern of adynamic bone is diminished bone quality and an increase in fracture risk. Our current study aims to investigate how bone quality changes with age in our previously established mouse model of adynamic bone. Young and old mice (4 months old and 16 months old, respectively) were used in this study. Col2.3Δtk (DTK) mice were treated with ganciclovir and pamidronate to create the adynamic bone condition. Bone quality was evaluated using established techniques including bone histomorphometry, microcomputed tomography, quantitative backscattered electron imaging, and biomechanical testing. Changes in mineral and matrix properties were examined by powder X-ray diffraction and Raman spectroscopy. Aging controls had a natural decline in bone formation and resorption with a corresponding deterioration in trabecular bone structure. Bone turnover was severely blunted at all ages in adynamic animals, which preserved trabecular bone loss normally associated with aging. However, the preservation of trabecular bone mass and structure in old adynamic mice did not rescue deterioration of bone mechanical properties. There was also a decrease in cortical bone toughness in old adynamic mice that was accompanied by a more mature collagen matrix and longer bone crystals. Little is known about the effects of metabolic bone disease on bone fracture resistance. We observed an age-related decrease in bone toughness that was worsened by the adynamic condition, and this decrease may be due to material level changes at the tissue level. Our mouse model may be useful in the investigation of the mechanisms involved in fractures occurring in elderly patients on antiresorptive therapy who have very low bone turnover. © 2015 American Society for Bone and Mineral Research.

KEY WORDS: AGING; COLLAGEN; BONE MATRIX; BIOMECHANICS; ORTHOPEDICS; ANTIRESORPTIVES; THERAPEUTICS

Introduction

Adynamic bone is defined histologically by very low or absent bone formation in association with thin osteoid seams, decreased cellularity (osteoblasts and osteoclasts), and minimal marrow fibrosis.[1,2] The pathogenesis of the adynamic bone condition is multifactorial, but the cellular hallmark of adynamic bone is a loss of bone turnover characterized by reductions in bone formation and resorption.[1] The adynamic bone condition is an increasingly common occurrence in patients with chronic kidney disease (CKD).[3,4] It represents 50% of all CKD-related mineral and bone disorders (MBDs) in patients on peritoneal dialysis, 19% in hemodialysis patients, and 16% in children with CKD-MBD.[5] However, there are many risk factors for low bone turnover aside from advanced CKD, such as advanced age, glucocorticoid-induced osteoporosis, diabetes, and hypoparathyroidism.[1,2] Long-term use of antiresorptives has been suspected to play a role in severely suppressed bone turnover,[6] and the combined effects of long-term antiresorptives and age-related decline in bone formation may lead to the adynamic bone condition.

Severely suppressed bone turnover is of clinical concern when considering the bone quality and fracture risk of elderly patients. Adynamic bone is associated with a reduced ability to repair damage from microfracture and from frank bone fracture, resulting in poor skeletal health and an increased risk of bone fragility and pain.[2] Two studies have suggested an increased risk of fracture in adynamic bone.[7,8] In the past decade, there

Received in original form December 29, 2014; revised form August 16, 2015; accepted August 29, 2015. Accepted manuscript online September 02, 2015.
Address correspondence to: Marc D Grynpas, PhD, Lunenfeld-Tanenbaum Research Institute, Mount Sinai Hospital, 60 Murray Street, Box 42, Toronto, Ontario, M5T 3L9, Canada. E-mail: grynpas@lunenfeld.on.ca

Journal of Bone and Mineral Research, Vol. xx, No. xx, Month 2015, pp 1–11
DOI: 10.1002/jbmr.2702
© 2015 American Society for Bone and Mineral Research

have been increasing concerns regarding the effects of long-term bisphosphonate use on bone metabolism.[9,10] Long-term use of bisphosphonates may suppress bone turnover to the point where bone remodeling and repair becomes impaired.[6,11]

Our laboratory previously established a novel mouse model of adynamic bone that directly targeted the actions of osteoblasts and osteoclasts.[12] In the current study, we used our mouse model of adynamic bone to explore how aging further compounds a state of low bone turnover because little is known about the effects of metabolic bone disease on bone toughness.

Materials and Methods

Animals

Col2.3Δ-TK (DTK)-positive and DTK-negative mice were used for this study. The mice were genotyped using the primers 5′HSV dTK: 5′-ACC TTA TGG GCA GCA TGA CCC-3′ and 3′HSV dTK: 5′-ACC ATC CCG GAG GTA AGT TGC-3′. All mice were housed at the Toronto Centre for Phenogenomics (TCP) with five mice to a cage under standard conditions with standard mouse chow (Teklad Global 18% Protein Rodent Diet, Harlan Laboratories, Madison, WI, USA).

Tissue-targeted transgenic expression of herpes simplex virus thymidine kinase (HSV-tk) has been used to conditionally ablate specific cell populations.[4,5] In brief, the DTK transgenic mouse expresses a truncated version of the HSV-tk gene (Δtk) driven under a 2.3-kb fragment of the rat type I collagen α1 (Col1a1) promoter.[13,14] To create the adynamic bone condition, female Col2.3Δ-TK (DTK) mice were treated with ganciclovir (GCV) and pamidronate to mimic loss of bone turnover as described.[12] GCV depleted differentiated osteoblasts to prevent bone formation while pamidronate inhibited bone resorption by osteoclasts. Two age groups were used in this study: 4-month-old and 16-month-old animals representing young and old animals, respectively. All animals were euthanized at the end of the treatment period and bones were harvested for bone quality assessments. A total of 45 mice were used in this study. All animal care procedures were reviewed and approved by TCP.

Preparation of bones

At euthanasia, the L_3 and L_4 vertebrae were excised and immediately immersed in a fixative. The L_3 vertebrae were fixed in 70% ethanol at room temperature for 5 days, then dehydrated in graded acetone and processed for embedding in Spurr's resin. Coronal sections were cut using a Leica RM2265 rotary microtome (Leica Microsystems, Richmond Hill, Ontario, Canada) for static and dynamic bone histomorphometry. The L_4 vertebrae were fixed in 10% neutral-buffered formalin, decalcified in EDTA (0.5 M, pH 7.4) at 4°C, and then processed in a graded formalin–ethanol series before embedding in paraffin. Five-μm-thick coronal sections were cut with a Leica Reichert Jung 2030 microtome and used for tartrate-resistant acid phosphatase (TRAP) staining of osteoclasts with an acid phosphatase leukocyte kit (Sigma-Aldrich, St. Louis, MO, USA) according to the manufacturer's instructions. Right and left femurs and L_5 and L_6 vertebrae were also excised, cleaned of adherent soft tissue, and stored at –20°C in saline-soaked gauze. This set of bones was thawed at room temperature before experimental testing.

Histology

Static and dynamic histomorphometric parameters of bone formation and resorption were evaluated on coronal sections of the L_3 vertebrae stained with Goldner's trichrome (5-μm-thick sections), or left unstained for calcein fluorescence (7-μm-thick sections). Five-μm-thick coronal sections of decalcified L_4 vertebra were stained for TRAP as an indirect indicator of bone resorption through the measurement of osteoclast number and surface. All histomorphometric measurements were expressed following the guidelines of the American Society of Bone and Mineral Research.[15,16]

Bone mineral densitometry and morphometry

The femurs and L_5/L_6 vertebral bodies were evaluated for areal bone mineral density (aBMD) by dual energy X-ray absorptiometry (DXA) using a PIXImus Bone Densitometer designed for small animal bone analyses (Lunar GE Corp., Mississauga, Ontario, Canada). Micro–computed tomography (μCT) (Skyscan 1174; Skyscan, Kontich, Belgium) was performed to measure volumetric bone mineral density (vBMD; g/cm^3) and morphometry of the cortical and trabecular compartments of femurs and L_6 vertebrae. Mid-diaphysis femurs were scanned in saline at a voxel size of 14.5 μm^3 for cortical bone assessment and L_6 vertebral bodies were scanned in saline-soaked gauze at a voxel size of 6.1 μm^3 for trabecular bone assessment. Image acquisition was performed at 50 kV and 800 μA, with a 0.25-mm aluminum filter to reduce beam hardening. A set of two hydroxyapatite phantoms (0.25 g/cm^3 and 0.75 g/cm^3) were scanned and used to calibrate and compute vBMD. Reconstructed images obtained from the scanner were analyzed using the Skyscan CT-Analyzer software (version 1.5.0) with volumes of interest (VOIs) established as follows: 1-mm VOI at the mid-diaphyseal cortical shell for femurs and a VOI between the growth plates for vertebrae. At the femoral midshaft, cortical bone area (B.Ar, mm^2), cortical thickness (μm), polar moment of inertia (J, mm^4), anteroposterior and mediolateral (AP, ML; mm) diameters were measured. In L_6 vertebrae, trabecular measurements included the bone volume fraction (BV/TV, %), trabecular thickness (Tb.Th, μm), trabecular number (Tb.N, mm^{-1}), and trabecular separation (Tb.Sp, μm).

Quantitative backscattered electron imaging

Quantitative backscattered electron imaging (qBEI) was used to analyze the bone mineral density distribution (BMDD) profiles of our animals. Spurr-embedded blocks of L_3 vertebrae used for histomorphometry were polished to a 1-μm diamond finish (Phoenix BETA Grinder/Polisher; Buehler, Whitby, Ontario, Canada), carbon-coated and imaged using a scanning electron microscope (XL30 SEM; FEI Company, Hillsboro, OR, USA), with the polished surface perpendicular to the incident beam set at an accelerating voltage of 20 kV, a load current of 4 nA, a beam spot size of 6.2, and a working distance of 15-mm. A backscattered electron (BSE) detector (solid state BSE detector; FEI Company) was used to image the entire polished bone surface at ×200 magnification. Calibration of the machine was performed with two standards: silicon dioxide (SiO_2) and magnesium fluoride (MgF_2). Different degrees of mineralization appeared as varying shades of gray in the image, and the contrast was set such that the nonmineralized tissue appeared black. Gray levels, ranging from 0 to 255, were used to describe the mineralization intensity, and histograms of the gray level

distribution were created where the higher the gray value the more mineralized the sample (mineralization peak). The full-width at half-maximum height (FWHM) of the histogram describes the mineral heterogeneity in the sample. A cumulative log ratio known as the logit function was used to evaluate shifts in the mineralization profile.[17] The logit function was calculated using Eq. 1. The "area" refers to the total bone fraction area defined within a specific mineralization range, and a gray level value of 180 was chosen as the "cutoff" value because it was the average mineralization peak of our control mice.

$$\text{logit} = \ln\left(\frac{area \leq cutoff}{area \geq cutoff}\right) \quad (1)$$

Biomechanical testing

Three-point bending was performed on the excised right femurs of all mice to test the biomechanical properties of cortical bone. Vertebral compression was performed on the excised L_6 vertebral bodies to test the biomechanical properties of trabecular bone undergoing a constant compressive stress. Femoral neck fracture testing represents a clinically relevant test that attempts to mimic the hip fracture. Femoral necks consist of both cortical and trabecular bone and possess a complex geometry. This test was performed on the proximal half of the right femurs previously fractured by three-point bending.

All biomechanical tests were performed on the Instron 4465 mechanical testing machine (Instron Corp., Canton, MA, USA) with a 100-N load cell applied at a constant rate of 1.0 mm/min until failure. Resulting load-deformation curves were generated on LabView 5.0 data acquisition software (National Instruments Corp., Austin, TX, USA) and ultimate load (N), yield load (N), energy to fail (mJ), and stiffness (N/mm) were measured. Normalized parameters ultimate stress (MPa), yield strain (MPa), toughness (J/mm^3), and Young's elastic modulus (MPa) were computed using the relevant femoral and vertebral geometry measured from μCT.[18]

Bone powder preparation

Left and right humeri from 4-month-old and 16-month-old animals were washed by vortexing three times in 0.2 M Tris-HCl (pH 7.4) containing the following protease inhibitors (PIs): benzamidine (5 mM); N-ethylmaleimide (5mM); ε-amino-n-caproic acid (10 mM), and phenylmethylsulfonyl fluoride (PMSF) (0.1 M), and then dried overnight (Automatic Environmental SpeedVac AES1000; Savant). Samples were then defatted in a 2:1 chloroform:methanol mixture and left to agitate for 24 hours at room temperature. Defatted samples were placed in 100% methanol for 1 hour and left to dry overnight. Dried samples were ground to a fine powder using a cryogenic freezer mill (SPEX certiprep 6750 Freezer Mill; Metuchen, NJ, USA). The bone powder was used for X-ray diffraction.

Powder X-ray diffraction

Powder X-ray diffraction (XRD) was used to evaluate crystal size and changes in overall crystallinity on ground mouse humeri. Peak broadening in bone XRD scans is largely due to the small crystal size of bone apatite and inherent lattice strain effects. The measurement of this peak broadening can then be related to the average crystal size/strain.[19] Each powdered sample was spread into a thin even layer on a quartz crystal sample holder. Using CuKα radiation at 40 kV and 40 mA, samples were scanned from 24.5 to 27.0 degrees (2θ) at a scan speed of 0.1 degrees per minute for crystal length (002) determination. Additionally, samples were scanned from 37.0 to 42.0 degrees (2θ) at a scan speed of 0.05 degrees per minute for crystal cross-section (310) analysis. Crystallite size was calculated from the peak broadening of the powder XRD peaks.[20] This broadening can be estimated by measuring the FWHM of each of the apatite peaks—$\beta_{1/2}$ (002) and $\beta_{1/2}$ (310)—using an Excel array formula. The effect of instrument broadening on peak broadening (β) was adjusted by using values obtained by scanning reference silicon at 26 and 55 degrees (2θ). The corrected sample broadening ($\beta_{1/2}$) was calculated as:

$$\beta_{1/2=}\sqrt{\beta^2(\text{specimen}) - \beta^2(\text{instrument})} \quad (2)$$

This corrected $\beta_{1/2}$ was used to calculate the crystalline size between the (002) and (310) planes using the Debye-Scherrer equation:

$$D = \frac{57.3k\lambda}{\beta_{1/2}\cos\theta} \quad (3)$$

where 57.3 is a conversion factor from degrees to radians, K is a correction factor (0.9) used to reflect the elongated apatite crystals of bone, λ is the K-emission wavelength of copper, θ is the diffraction angle, and D is the size of the crystallite in angstroms along the specific axis.

Raman spectroscopy

The chemical composition of bone samples was assessed by exploiting a WITec Alpha 300 confocal Raman microscope (WITec, Germany). A 532-nm frequency-doubled Nd:YAG laser (WITec, Germany) was used to probe samples at a power of 7.3 mW measured at the 20× air objective. Three spectra per sample were collected in randomly selected regions of the cortical bone on the cross-section in the midshaft of the left femur. Two acquisitions with an integration time of 60 s each was used to enhance the signal-to-noise ratio. The analyses was confined to the Raman scattering region between 800 and 1800 cm^{-1}.

Raman data were processed by the OriginPro software (OriginLab Corporation, USA). Raman spectra were fitted by Gaussian functions after linear baseline subtraction. Peak assignment and interpretation were carried out according to the literature.[21,22] Commonly used Raman bone metrics were calculated: mineral-to-matrix ratio (phosphate ν_1-to-amide I, 959 cm^{-1}/1665 cm^{-1}; phosphate ν_1-to-amide III, 959 cm^{-1}/1270 cm^{-1}; phosphate ν_1-to-CH_2 scissoring, 959 cm^{-1}/1450 cm^{-1}), carbonate substitution ratio (phosphate ν_1-to-carbonate, 959 cm^{-1}/1070 cm^{-1}), crystallinity (phosphate ν_1 inverse FWHM at ~959 cm^{-1}), and collagen crosslink ratio using the ratio of the amide I sub-bands (1665 cm^{-1}/1685 cm^{-1}).

Statistical analyses

Data are presented as mean ± standard deviation (SD), unless otherwise stated. All results were analyzed using SPSS 17.0 statistical analyses software (SPSS Inc., Chicago, IL, USA). Two-way analyses of variance (ANOVA) was conducted to investigate the independent and interactive effects of age and the adynamic bone condition on measured parameters. The

data was considered to be statistically significant at a confidence level of 95% ($p = 0.05$).

Results

Bone turnover

We have previously established that our mouse model of adynamic bone has similar histology to the human condition and severe suppression of bone formation and resorption in the vertebrae and tibia.[8] There was a natural decline in bone formation and resorption in aging controls, but bone turnover was blunted at all ages in adynamic animals (Fig. 1, Table 1).

BMD and microarchitecture

There were no differences in aBMD or vBMD in the femur or vertebrae between control and adynamic animals at any age. The cross-sectional bone area of the femoral midshaft increased with age without an increase in cortical thickness for both control and adynamic animals (Table 2), which is most likely a result of continued periosteal apposition and endosteal resorption with aging. The trabecular compartment of the vertebral body in 16-month-old adynamic animals had a higher vBMD than the trabecular compartment of 16-month-old control animals (Table 2). This difference in trabecular vBMD reflected significant deterioration in trabecular microarchitecture in 16-month-old control animals as a function of aging (Fig. 2, Table 2).

Bone mechanical properties

We performed compression tests on the L_6 vertebral bodies and three-point bending tests on the right femurs to investigate the effects of aging and adynamic condition on bone mechanical properties. Vertebral compression tests showed that regardless of treatment the L_6 vertebral bodies of old animals had a lower failure displacement (–90%), energy to failure (up to –65%), normalized failure strain (–90%), and toughness (–90%); but an increase in stiffness (30%) and normalized Young's modulus (50%) compared to young animals (Table 3, Fig. 3). Three-point bending tests on the right femur showed a different ageing pattern in cortical bone mechanical properties between controls and adynamic animals. Our data showed that there were no significant differences in cortical bone mechanical properties between young and old control animals after normalization for geometry. However, the femurs of old adynamic animals had a significant decrease in failure displacement (–45%), energy to failure (–31%), normalized failure strain (–38%), and toughness (–38%) (Table 4, Fig. 4). μCT scans were conducted on the vertebral bodies and femurs prior to mechanical testing; therefore, samples may have experienced possible irradiation damage and may have shifted absolute values of the testing parameters.

The femoral neck region of the proximal end of the excised right femur was also tested to failure in an attempt to evaluate bone mechanical properties at a clinically relevant site. Peak force loads were collected and compared. There were no differences in the peak force load between control and adynamic animals at 4 months or 16 months (data not presented).

BMD distribution

qBEI of the L_3 vertebrae detected changes in the homogeneity of the BMDD, as represented by the FWHM of the histogram. Overall, the adynamic bone condition decreased the FWHM by

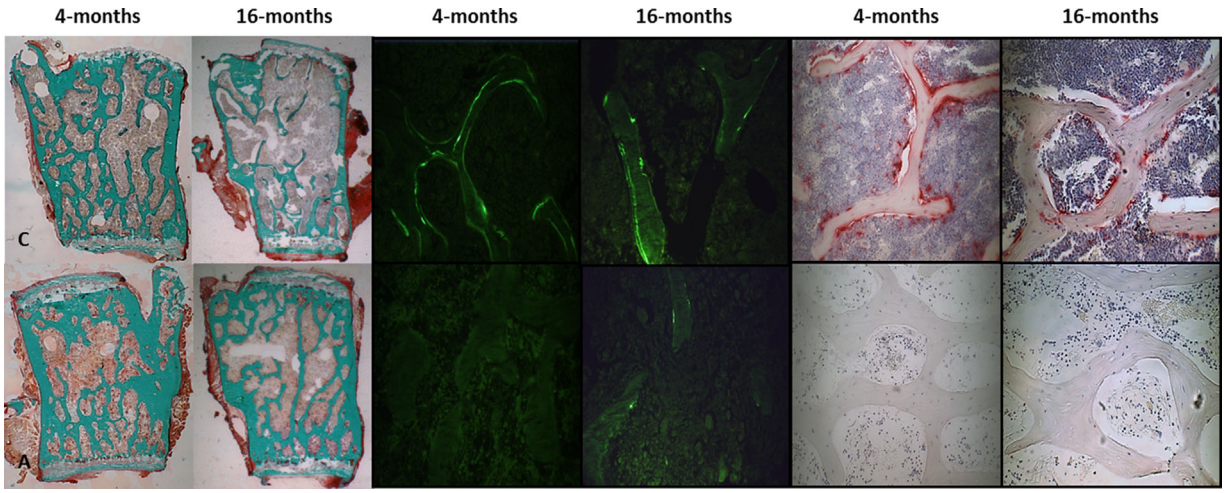

Fig. 1. Changes in bone histology with age in the vertebrae. Control animals (labeled "C") are presented in the top row and adynamic animals (labeled "A") are presented in the bottom row. Young animals are 4 months of age, and old animals are 16 months of age. (Left) Bone structure and cellularity: undecalcified Goldner's trichrome-stained 5-μm sections (×25). Old control mice decreased in trabecular bone volume compared to young control mice, but old adynamic mice preserved their trabecular bone volume. (Middle) Bone formation: undecalcified, unstained 7-μm sections (×400); calcein green was injected intraperitoneally 10 and 2 days prior to euthanasia. Old control mice showed a decrease in calcein labeling, but bone formation was blunted in adynamic mice regardless of age. (Right) TRAP-positive osteoclasts (black arrows): decalcified, TRAP-stained 5-μm sections (×400). Old control mice showed a decrease in TRAP-positive osteoclasts but adynamic mice showed a profound reduction in osteoclasts at all ages. (Note: Four-month-old data reprinted from "Development, validation and characterization of a novel mouse model of adynamic bone disease (ABD), " Ng et al., 2014, Bone, 68, p. 60. Copyright 2014 by Elsevier B.V. Adapted with permission.)

Table 1. Changes in Bone Turnover Measured by Histomorphometry

	4 months old (young)		16 months old (old)	
	Control ($n = 11$)	Adynamic ($n = 10$)	Control ($n = 8$)	Adynamic ($n = 10$)
BV/TV (%)	17.85 ± 4.36	22.30 ± 7.70	14.43 ± 5.41	20.10 ± 9.32
OV/BV (%)	$0.31 \pm 0.27^{**}$	0.05 ± 0.06	$0.04 \pm 0.02^{*,**}$	0.002 ± 0.004
OS/BS (%)	$4.42 \pm 3.59^{**}$	0.59 ± 0.78	$0.43 \pm 0.23^{*}$	0.03 ± 0.05
MAR	10.23 ± 5.66	0.00	0.83 ± 0.10	0.00
BFR (μm/day)	$0.30 \pm 0.09^{**}$	0.00	$0.18 \pm 0.08^{*,**}$	0.00
N.Oc/BS	$5.51 \pm 1.64^{**}$	0.06 ± 0.05	$3.06 \pm 1.11^{*,**}$	0.15 ± 0.20

Four-month-old data reprinted from "Development, validation and characterization of a novel mouse model of adynamic bone disease (ABD)," Ng et al., 2014, Bone, 68, p. 60. Copyright 2014 by Elsevier B.V. Adapted with permission.

BV/TV = bone volume; OV/TV = osteoid volume; OS/BS = osteoid surface/bone surface; MAR = mineral apposition rate; BFR = bone formation rate; N.Oc/BS = number of osteoclasts.

$^{*}p < 0.05$ relative to 4-month-old control.

$^{**}p < 0.01$ relative to adynamic within its age group.

9% when compared to control mice ($p < 0.001$), indicative of a more homogenous BMDD. There was no difference in BMDD between young and old control mice (Table 5). We used the logit function as a parameter to assess skewedness of the mineralization profiles. The closer the logit function is to zero, the more normally distributed the mineralization profile appears. Negative logit functions represent skewed hypermineralization distributions, whereas positive logit functions represent skewed hypomineralized distributions. Adynamic animals had a more hypermineralized distribution compared to control animals regardless of age ($p < 0.05$). The adynamic bone condition increased the mean degree of bone mineralization by 20% at 4 months and 30% by 16 months as measured by the logit function (Fig. 5).

Bone crystal size

There was no difference in crystallite cross-section (310) between old or young animals (Table 6); however, old adynamic animals had 13% longer crystallite lengths along the c-axis (002) than young adynamic animals, $p = 0.09$ (Table 6).

Bone composition

Various ratios were calculated from the Raman spectra to describe changes to the mineral and matrix composition (Fig. 6). In our analyses there was no difference in carbonate substitution with treatment or age. There was a main effect of age in the mineral-to-matrix ratio ($p < 0.05$) and crystallinity ($p < 0.01$), where old (16-month-old) animals had a higher mineral-to-matrix ratio and crystallinity compared to young (4-month-old) animals. Collagen maturity was described by the collagen crosslink ratio using the amide I sub-bands at $\sim 1665\,cm^{-1}$ and $\sim 1685\,cm^{-1}$. The component at $\sim 1665\,cm^{-1}$ corresponds to pyridinoline (PYD) crosslinked peptides. PYD is a mature, trivalent, nonreducible crosslink. The component at $\sim 1685\,cm^{-1}$ corresponds to dehydrodihydroxylysinonorleucine (DPD), which is an immature, divalent, reducible crosslink.

Table 2. Changes in Bone Mineral Density and Microarchitecture Measured by μCT

	4 months old (young)		16 months old (old)	
	Control ($n = 10$)	Adynamic ($n = 11$)	Control ($n = 8$)	Adynamic ($n = 10$)
Femur midshaft				
Cortical vBMD (g/cm^3)	1.24 ± 0.03	1.24 ± 0.02	$1.26 \pm 0.03^{*,**}$	$1.27 \pm 0.03^{*,**}$
Cortical thickness (mm)	0.23 ± 0.02	0.24 ± 0.02	0.25 ± 0.02	0.27 ± 0.06
Cross-sectional bone area (mm^2)	1.02 ± 0.09	1.06 ± 0.11	$1.17 \pm 0.13^{*}$	$1.23 \pm 0.25^{***}$
Vertebrae				
Whole vertebrae vBMD (g/cm^3)	0.39 ± 0.04	0.38 ± 0.06	0.38 ± 0.07	0.44 ± 0.10
Trabecular vBMD (g/cm^3)	0.39 ± 0.05	0.32 ± 0.06	$0.27 \pm 0.07^{***}$	0.36 ± 0.12
BV/TV (%)	22.98 ± 3.02	25.18 ± 3.55	$16.66 \pm 4.54^{*,***}$	23.78 ± 8.76
Tb.Th (μm)	63.74 ± 2.78	64.78 ± 3.66	$65.40 \pm 6.21^{***}$	$70.75 \pm 6.25^{**}$
Tb.N (1/mm)	3.60 ± 0.39	3.89 ± 0.51	$2.52 \pm 0.48^{*,***}$	$3.30 \pm 1.00^{**}$
Tb.Sp (mm)	0.27 ± 0.03	0.25 ± 0.04	$0.33 \pm 0.04^{*,***}$	0.28 ± 0.06

Four-month-old data reprinted from "Development, validation and characterization of a novel mouse model of adynamic bone disease (ABD)," Ng et al., 2014, Bone, 68, p. 60. Copyright 2014 by Elsevier B.V. Adapted with permission.

vBMD = volumetric bone mineral density; BV/TV = bone volume; Tb.Th = trabecular thickness; Tb.N = trabecular number; Tb.Sp = trabecular separation.

$^{*}p < 0.05$ relative to 4-month-old control.

$^{**}p < 0.05$ relative to 4-month-old adynamic.

$^{***}p < 0.01$ relative to 16-month-old adynamic.

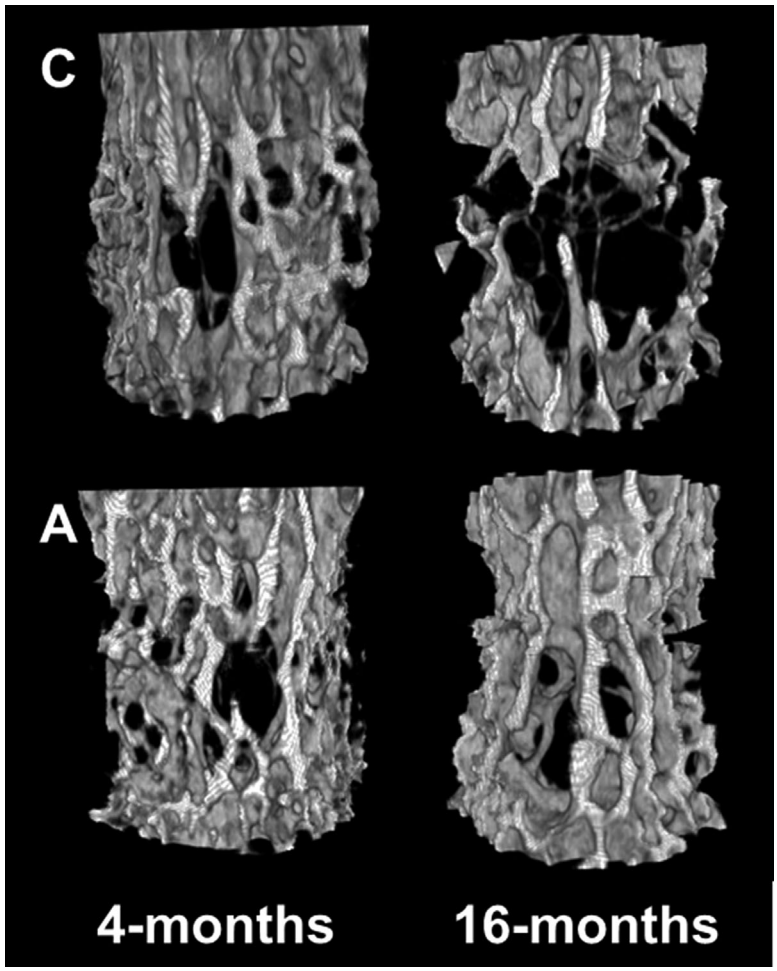

Fig. 2. Changes in bone microarchitecture in the vertebrae. Representative μCT 3D renderings of the L_6 vertebrae. Control animals (labeled "C") showed a decline in trabecular bone volume with age ($p < 0.05$) as well as deterioration in trabecular microarchitecture (decrease in trabecular number and increase in trabecular separation). Sixteen-month-old (old) adynamic animals (labeled "A") preserved trabecular bone volume and microarchitecture.

Table 3. Changes in Vertebral Biomechanical Properties: Vertebral Compression Tests

	4 months old (young)		16 months old (old)	
	Control ($n = 9$)	Adynamic ($n = 11$)	Control ($n = 9$)	Adynamic ($n = 10$)
Structural properties				
Ultimate load (N)	20.7 ± 8.4	24.9 ± 6.9	19.0 ± 7.3	24.5 ± 13.5
Failure displacement (mm)	0.47 ± 0.20	$0.29 \pm 0.04^{*}$	$0.02 \pm 0.06^{*}$	$0.02 \pm 0.06^{**}$
Energy to failure (mJ)	6.9 ± 4.7	4.6 ± 1.7	$2.4 \pm 1.7^{*}$	3.4 ± 2.6
Stiffness (N/mm)	117 ± 67	164 ± 59	164 ± 61	209 ± 112
Material properties				
Ultimate stress (MPa)	20.6 ± 5.6	21.2 ± 5.4	20.5 ± 5.6	22.2 ± 7.8
Failure strain (%)	14.3 ± 6.1	$8.6 \pm 1.3^{*}$	$5.0 \pm 2.1^{*}$	$5.8 \pm 1.0^{**}$
Toughness (J/mm^3)	2.1 ± 1.1	$1.2 \pm 0.5^{*}$	$0.1 \pm 1.9^{*}$	$0.1 \pm 3.8^{**}$
Young's modulus (GPa)	0.38 ± 0.18	0.46 ± 0.11	$0.74 \pm 0.17^{*}$	$0.71 \pm 0.22^{**}$

Four-month-old data reprinted from "Development, validation and characterization of a novel mouse model of adynamic bone disease (ABD)," Ng et al., 2014, Bone, 68, p. 60. Copyright 2014 by Elsevier B.V. Adapted with permission.

$^{*}p < 0.05$ relative to 4-month-old control.

$^{**}p < 0.05$ relative to 4-month-old adynamic.

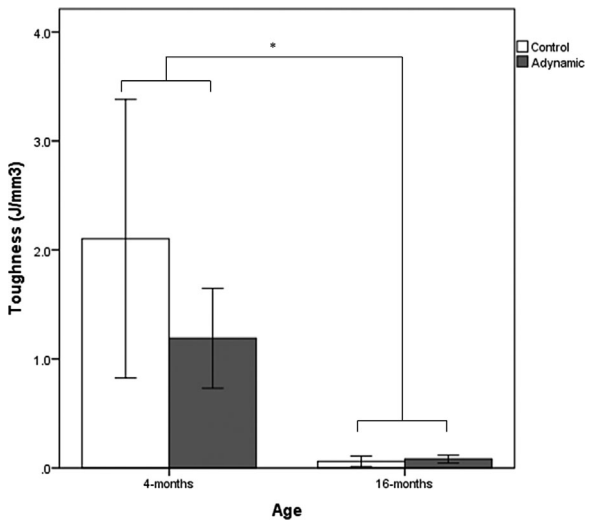

Fig. 3. Changes in vertebral biomechanical properties with age. In vertebral compression testing of the L_6 vertebrae, there were no differences between control and adynamic animals within each age group. Regardless of treatment, 16-month-old (16-months, old) animals required significantly less energy to failure, $^{*}p < 0.05$.

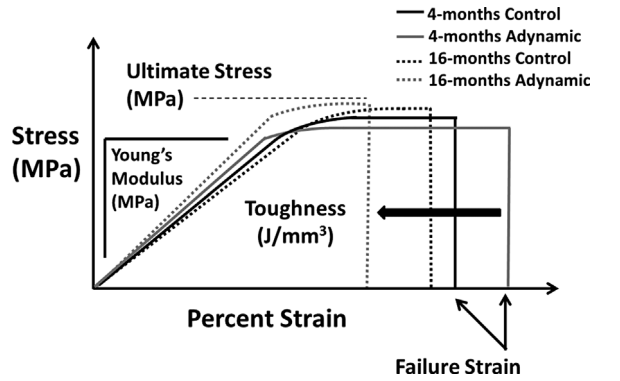

Fig. 4. Changes in cortical bone toughness with age. In three-point bending of the right femur, 16-month-old (16-months, old) adynamic mice required significantly less energy to failure (toughness) than 4-month-old (4-months, young) adynamic mice (black arrow), $p < 0.05$. There was no difference between young and old control animals.

In general, adynamic animals tended to have a higher collagen crosslink ratio than control animals (+12%, $p = 0.097$), and old animals had more mature collagen crosslinks than young animals (+41%, $p < 0.001$). Finally, there was an interaction between age and treatment, with old adynamic mice having ~68% more mature collagen crosslinks compared to young adynamic mice ($p < 0.001$) and ~31% more compared to old control mice ($p < 0.01$).

Discussion

We previously developed a mouse model to investigate changes to bone quality in the adynamic bone condition.[12] Our previous study showed that at 4 months of age, the adynamic bone condition in our mouse altered the bone material and structural properties and shifted the bone to a more hypermineralized profile.[12] In the current study, we investigated the effects of increasing age on bone quality and how suppressed bone turnover further compounds the aging process on bone quality.

Laboratory mice do not experience natural osteoporosis, but a decrease in bone mass accompanying advancing age has been observed.[23] Histomorphometry and μCT analyses confirmed this age-related pattern of bone loss in the vertebrae of our old control animals, whereas a loss of bone turnover in the adynamic bone condition prevented this age-related bone loss. We assume this age-related decline in bone turnover applies to other skeletal sites, such as the tibia, as suggested by our previous study.[12]

The strength of bone is determined by its material composition and structure.[24–26] Old adynamic animals had a higher BV/TV than old control animals, as well as a better-connected

Table 4. Changes in Femoral Biomechanical Properties: Three-Point Bend Tests

	4 months old (young)		16 months old (old)	
	Control ($n = 10$)	Adynamic ($n = 11$)	Control ($n = 7$)	Adynamic ($n = 10$)
Structural properties				
Ultimate load (N)	24.9 ± 1.9	25.6 ± 2.3	$35.0 \pm 3.1^{*}$	$37.2 \pm 9.1^{**}$
Failure displacement (mm)	0.42 ± 0.10	$0.49 \pm 0.09^{*}$	$0.32 \pm 0.06^{*}$	$0.27 \pm 0.05^{**}$
Energy to failure (mJ)	7.51 ± 1.82	$9.28 \pm 1.46^{*}$	7.79 ± 1.74	$6.42 \pm 2.10^{**}$
Stiffness (N/mm)	199 ± 20	197 ± 27	$273 \pm 40^{*}$	$276 \pm 46^{**}$
Material properties				
Ultimate stress (MPa)	153.9 ± 16.6	150.5 ± 16.2	166.3 ± 21.7	178.2 ± 17.4
Failure strain (%)	9.3 ± 2.2	10.8 ± 1.7	8.2 ± 1.8	$6.7 \pm 1.4^{**}$
Toughness (J/mm^3)	10.3 ± 2.1	12.0 ± 1.8	9.3 ± 2.2	$7.5 \pm 2.4^{**}$
Young's modulus (GPa)	5.6 ± 1.0	5.3 ± 1.0	5.2 ± 1.1	5.6 ± 0.7

Four-month-old data reprinted from "Development, validation and characterization of a novel mouse model of adynamic bone disease (ABD)," Ng et al., 2014, Bone, 68, p. 60. Copyright 2014 by Elsevier B.V. Adapted with permission.

$^{*}p < 0.05$ relative to 4-month-old control.

$^{**}p < 0.05$ relative to 4-month-old adynamic.

Table 5. Results From BSE Imaging of Mice Vertebrae

	4 months old (young)		16 months old (old)	
	Control ($n = 11$)	Adynamic ($n = 11$)	Control ($n = 7$)	Adynamic ($n = 8$)
Logit	$-1.36 \pm 0.25^{*}$	-1.61 ± 0.10	$-1.37 \pm 0.36^{*}$	-1.78 ± 0.19
Peak gray level	192 ± 10	187 ± 9	$190 \pm 10^{*}$	$203 \pm 11^{**}$
FWHM	34 ± 4	$28 \pm 3^{*}$	37 ± 3	$35 \pm 4^{**}$

Four-month-old data reprinted from "Development, validation and characterization of a novel mouse model of adynamic bone disease (ABD)," Ng et al., 2014, Bone, 68, p. 60. Copyright 2014 by Elsevier B.V. Adapted with permission.

BSE = backscattered electron; FWHM = full-width at half-maximum height of mineralization histogram.

$^{*}p < 0.05$ relative to adynamic within its age group.

$^{**}p < 0.01$ relative to 4-month-old adynamic.

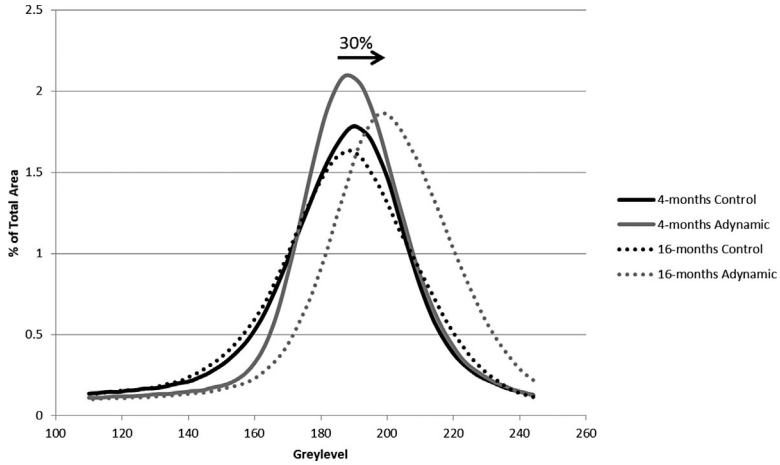

Fig. 5. Changes in the mean degree of bone mineral density. Adynamic bone decreased the heterogeneity of the bone mineral density distribution by 9%, $p < 0.001$. Adynamic animals had a higher mean degree of bone mineralization compared to control animals regardless of age, $p < 0.05$, as illustrated by the shift of the logit function to the right by 20% at 4 months and 30% by 16 months.

trabecular structure. These bone quality parameters collectively suggested maintenance of bone mechanical properties in old adynamic animals. However, our data showed that high BMD and a well-connected trabecular network do not necessarily equate bones that can withstand a higher mechanical load. More importantly, BMD alone may not be a good metric of bone health in adynamic bone, especially at an advanced age. Bone quality is a function of its structural and material properties that are influenced by bone turnover.[24,26] Because the preservation of bone mass and structure in old adynamic animals did not rescue the decrease in bone mechanical properties in advanced age, we hypothesized that bone quality deterioration must be in part attributed to compositional changes in aged adynamic animals. To test our hypothesis, we further investigated the material and composition properties of bones from adynamic animals.

Bisphosphonate treatment has been documented to decrease the heterogeneity of the bone mineral distribution[27–29] as well as increase the mean degree of mineralization in bone.[29,30] These phenomena are presumably based on the ability of bisphosphonates to suppress osteoclastic resorption and decreasing bone turnover over time,[30,31] and the effects of bisphosphonates are likely to be more pronounced in the trabecular compartment than cortical compartment due to increased surface area and metabolic activity. As illustrated in Fig. 5, aging tended to increase the heterogeneity of the mineral distribution,[27] whereas the adynamic bone condition decreased the heterogeneity of the mineral distribution independent of age. The effect of bone turnover suppression was so strong in old adynamic animals that the entire mineral distribution was shifted toward a more hypermineralized profile

Table 6. Bone Mineral Crystal Length (002) and Bone Mineral Crystal Cross-Section (310), Estimated by Powder X-Ray Diffraction

	4 months old (young)		16 months old (old)	
	Control ($n = 11$)	Adynamic ($n = 11$)	Control ($n = 6$)	Adynamic ($n = 8$)
Bone mineral crystal length (Å)	152.6 ± 19.1	152.4 ± 17.9	152.2 ± 31.2	$170.6 \pm 19.3^{*}$
Bone mineral crystal width (Å)	76.0 ± 13.7	68.9 ± 18.8	74.3 ± 16.2	74.5 ± 9.9

$^{*}p = 0.09$ relative to 4-month-old adynamic.

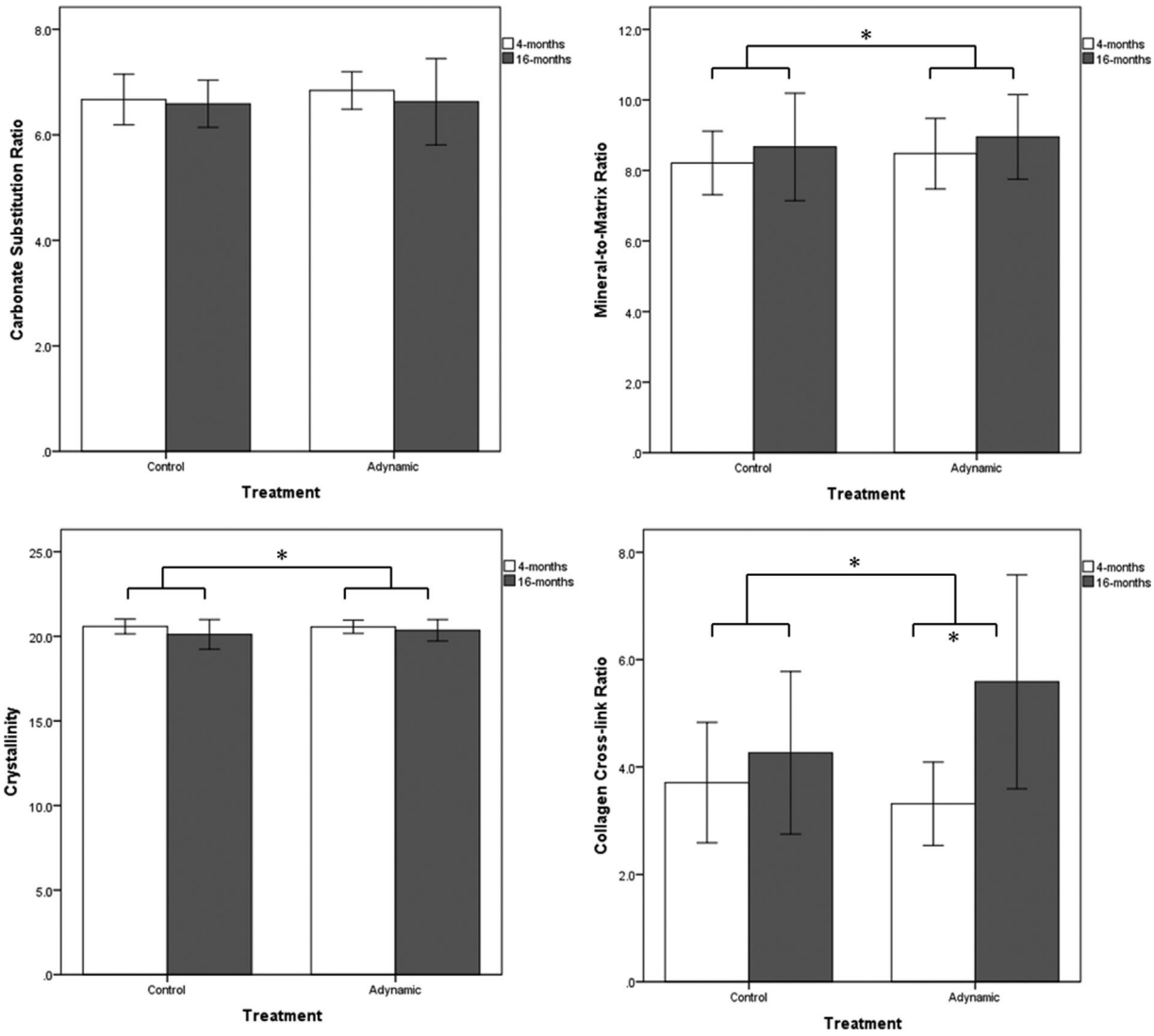

Fig. 6. Raman ratios of bone composition. Sixteen-month-old (16-months, old) animals had a significantly higher mineral-to-matrix ratio, collagen crosslink ratio, and crystallinity compared to 4-month-old (4-months, young) animals, $p < 0.05$. Old adynamic animals had a higher collagen crosslink ratio than young adynamic animals, $p < 0.05$, indicating a matrix that has more mature collagen crosslinks.

by 30% at 16 months old. qBEI data suggest that although BMD is preserved in old adynamic bones, the bones become more hypermineralized compared to old control bones.

Bone mineralization is a multistep process. Primary mineralization begins 5 to 10 days post–matrix deposition, which can be visualized using double fluorochrome labeling. Secondary mineralization is a slow and gradual process after primary mineralization has completed and leads to gradual maturation of the mineral component, including an increase in the amount of crystals and/or an increase in crystal size. We investigated whether bone crystal size was affected in the adynamic bone state to contribute to an increase in the mean degree of bone mineralization. Bone crystals from old adynamic mice were slightly longer compared to the bone crystals from controls and young adynamic mice. We suspect a lengthened secondary mineralization period due to suppressed bone turnover[31] allowed the crystals to grow in length along their (c-) axis in length in old adynamic mice.

Bone strength is a function of bone quantity, mineral density, and tissue material properties; bone turnover is an important determinant of these bone quality properties.[25] Bone is a two-phase composite material in which the mineral phase provides stiffness to resist deformation and the collagen matrix provides the flexibility that is required to absorb energy during compression and tension to resist cracking.[18,25] The increases in mean degree of bone mineralization and bone crystal length did not explain the decrease in bone toughness observed in our 16-month-old adynamic mice. Raman spectroscopy confirmed the changes in bone mineral observed in our qBEI and XRD analyses. The shift to a hypermineralization distribution observed with qBEI is most likely the result of a higher mineral-to-matrix ratio and increased mineral crystallinity. In other words, ageing in adynamic bone created larger crystals[32] and more mineral per volume of matrix.[33–35] These changes in the bone mineral component accounted for the increase in ultimate stress and modulus we observed in our three-point

bending data, but these changes do not fully explain the loss of toughness in the vertebrae and femur.[36] Collagen crosslinks are another important component that affects bone mechanical properties. Therefore, we used Raman spectroscopy to investigate possible material-level changes to the composition of the organic matrix to further explain our bone mechanical testing results.[21,22]

Raman analysis revealed advancing age and bone turnover suppression resulted in a matrix that had a higher ratio of mature collagen crosslinks. The ratio of mature to immature crosslinks is a function of age and bone turnover.[37,38] Divalent immature crosslinks convert to mature crosslinks with age, and these stable mature crosslinks were not replaced with younger organic matrix because of a reduction in bone turnover.[28,39,40] Divalent immature crosslinks in the collagen matrix are important determinants of bone strength.[41] An animal study showed a reduction in immature divalent crosslinks decreased mechanical properties in femurs of diabetic rats.[41] A more mature collagen matrix may not be able to absorb or dissipate as much energy as a younger matrix with more immature crosslinks.[41,42]

Advancing age increased bone crystallinity and mineral-to-matrix ratio, resulting in a more hypermineralized tissue that may cause bones to become more brittle.[43] In addition, a suppressed state of bone turnover in the adynamic bone condition further contributed to the growth and maturation of the mineral component in bone, elongating the bone crystal and increasing the mean degree of bone mineralization. The same maturation pattern was also observed in the bone matrix, where the adynamic condition compounded the accumulation of mature collagen crosslinks associated with advanced age. The combined effect of adynamic bone and aging resulted in a phenotype that appeared normal or has better preserved bone mass and structure. In other words, standard methods of bone measurement to assess bone health, such as BMD and trabecular structure (pQCT) measurements, would predict that old adynamic bone to be stronger bones. However, the mechanical properties of the bones were profoundly decreased by aging and the adynamic bone condition, resulting in bones of poorer material quality. Thus, the overall bone toughness of old adynamic mice was compromised despite a normal BMD and structure.

We should mention that the adynamic mice in this study underwent daily GCV injections and weekly pamidronate injections for 6 weeks to achieve the adynamic bone condition. Both young (4-month-old) and old (16-month-old) adynamic animals experienced weight loss from these injections. We anticipated the weight loss would dampen the adynamic bone phenotype, especially in the 16-month-old animals, because weight loss can result in a reduction of bone mass. However, our adynamic animals maintained their BMD despite a reduction in weight from repeated injections. Therefore, the stress of daily injections and weight loss did not have an impact on the observed bone phenotype.

In conclusion, although our aging adynamic mice showed antiresorptive treatment had a protective effect on trabecular bone volume and microarchitecture, the preservation of these properties did not translate into improved biomechanical properties in the adynamic bone condition. Despite a normal BMD, the bones of aging adynamic mice were less tough than that of control mice, most notably in the cortical compartment, and this decrease may be due to changes beyond the mineral phase. This finding may reflect observations in the clinical setting where patients on long-term antiresorptive therapy experience atypical fractures in the subtrochanteric region in the femur shaft. Our adynamic bone mouse model may be useful in the investigation of the mechanisms involved in fractures occurring in elderly patients on antiresorptive therapy who have very low bone turnover. More importantly, our data suggest that current clinical diagnostic technique (ie, bone mineral density testing) and even trabecular structure may not provide a sufficient index for bone health in the adynamic bone condition. Additional research should focus on the aging matrix and its contribution to changes in bone biomechanical properties.

Disclosures

All authors state that they have no conflicts of interest.

Acknowledgements

This work was supported by a grant from the Canadian Institutes of Health Research (CIHR) (MOP-102479) to MDG and BAA. AHN was funded by scholarships from the University of Toronto, Lunenfeld-Tanenbaum Research Institute, Ontario Graduate Scholarship fund, and CIHR. We thank Puviindran Nadesan, Douglas Holmyard, George Kretschmann, Dr. Mircea Dumitriu, and Dr. Gurpreet Baht for their technical assistance. FV acknowledges funding from the Canada Foundation for Innovation (CFI), the Ontario Ministry of Research and Innovation, and the Natural Sciences and Engineering Research Council of Canada (NSERC).

Authors' roles: AHN, BAA, and MDG initiated the study and designed the experiments. AHN, SO, FV, BA, and TLW were involved in data collection and analysis. AHN and MDG wrote the manuscript.

References

1. Andress DL. Adynamic bone in patients with chronic kidney disease. Kidney Int. 2008;73(12):1345–54.
2. Brandenburg VM, Floege J. Adynamic bone disease—bone and beyond. NDT Plus. 2008;1(3):12.
3. Malluche HH, Mawad H, Monier-Faugere MC. The importance of bone health in end-stage renal disease: out of the frying pan, into the fire? Nephrol Dial Transplant. 2004;19 Suppl 1:i9–13.
4. Sherrard DJ, Hercz G, Pei Y, et al. The spectrum of bone disease in end-stage renal failure—an evolving disorder. Kidney Int. 1993;43(2):436–42.
5. Kidney Disease: Improving Global Outcomes (KDIGO) CKD-MBD Work Group. KDIGO clinical practice guideline for the diagnosis, evaluation, prevention, and treatment of chronic kidney disease-mineral and bone disorder (CKD-MBD). Kidney Int Suppl. 2009 Aug; (113):S1–130.
6. Odvina CV, Zerwekh JE, Rao DS, Maalouf N, Gottschalk FA, Pak CY. Severely suppressed bone turnover: a potential complication of alendronate therapy. J Clin Endocrinol Metab. 2005;90(3):1294–301.
7. Atsumi K, Kushida K, Yamazaki K, Shimizu S, Ohmura A, Inoue T. Risk factors for vertebral fractures in renal osteodystrophy. Am J Kidney Dis. 1999;33(2):287–93.
8. Piraino B, Chen T, Cooperstein L, Segre G, Puschett J. Fractures and vertebral bone mineral density in patients with renal osteodystrophy. Clin Nephrol. 1988;30(2):57–62.
9. Compston J. Over-suppression of bone turnover: does it exist? Curr Osteoporos Rep. 2007;5(4):179–85.
10. Schmidt GA, Horner KE, McDanel DL, Ross MB, Moores KG. Risks and benefits of long-term bisphosphonate therapy. Am J Health Syst Pharm. 2010;67(12):994–1001.

11. Visekruna M, Wilson D, McKiernan FE. Severely suppressed bone turnover and atypical skeletal fragility. J Clin Endocrinol Metab. 2008;93(8):2948–52.
12. Ng AH, Willett TL, Alman BA, Grynpas MD. Development, validation and characterization of a novel mouse model of adynamic bone disease (ABD). Bone. 2014;68:57–66.
13. Visnjic D, Kalajzic I, Gronowicz G, et al. Conditional ablation of the osteoblast lineage in Col2.3deltatk transgenic mice. J Bone Miner Res. 2001;16(12):2222–31.
14. Visnjic D, Kalajzic Z, Rowe DW, Katavic V, Lorenzo J, Aguila HL. Hematopoiesis is severely altered in mice with an induced osteoblast deficiency. Blood. 2004;103(9):3258–64.
15. Dempster DW, Compston JE, Drezner MK, et al. Standardized nomenclature, symbols, and units for bone histomorphometry: a 2012 update of the report of the ASBMR Histomorphometry Nomenclature Committee. J Bone Miner Res. 2013;28(1):2–17.
16. Parfitt AM, Drezner MK, Glorieux FH, et al. Bone histomorphometry: standardization of nomenclature, symbols, and units. Report of the ASBMR Histomorphometry Nomenclature Committee. J Bone Miner Res. 1987;2(6):595–610.
17. Bracci PM, Bull SB, Grynpas MD. Analysis of compositional bone density data using log ratio transformations. Biometrics. 1998;54(1):337–49.
18. Turner CH, Burr DB. Basic biomechanical measurements of bone: a tutorial. Bone. 1993;14(4):595–608.
19. Burr DB, Miller L, Grynpas M, et al. Tissue mineralization is increased following 1-year treatment with high doses of bisphosphonates in dogs. Bone. 2003;33(6):960–9.
20. Klug HP, Alexander LE. X-ray diffraction procedures for polycrystalline and amorphous materials. 2nd ed. New York: Wiley; 1974. 992 p.
21. Gourion-Arsiquaud S, Boskey AL. Fourier transform infrared and Raman microspectroscopy and microscopic imaging of bone. Curr Opin Orthop. 2007;18(5):499–504. DOI:10.1097/BCO.0b013e3282b97133.
22. Morris MD, Mandair GS. Raman assessment of bone quality. Clin Orthop Relat Res. 2011;469(8):2160–9.
23. Watanabe K, Hishiya A. Mouse models of senile osteoporosis. Mol Aspects Med. 2005;26(3):221–31.
24. Donnelly E. Methods for assessing bone quality: a review. Clin Orthop Relat Res. 2011;469(8):2128–38.
25. Seeman E, Delmas PD. Bone quality—the material and structural basis of bone strength and fragility. N Engl J Med. 2006;354(21):2250–61.
26. van der Meulen MC, Jepsen KJ, Mikic B. Understanding bone strength: size isn't everything. Bone. 2001;29(2):101–4.
27. Brennan MA, Gleeson JP, O'Brien FJ, McNamara LM. Effects of ageing, prolonged estrogen deficiency and zoledronate on bone tissue mineral distribution. J Mech Behav Biomed Mater. 2014;29:161–70.
28. Gourion-Arsiquaud S, Allen MR, Burr DB, Vashishth D, Tang SY, Boskey AL. Bisphosphonate treatment modifies canine bone mineral and matrix properties and their heterogeneity. Bone. 2010;46(3):666–72.
29. Roschger P, Rinnerthaler S, Yates J, Rodan GA, Fratzl P, Klaushofer K. Alendronate increases degree and uniformity of mineralization in cancellous bone and decreases the porosity in cortical bone of osteoporotic women. Bone. 2001;29(2):185–91.
30. Boivin GY, Chavassieux PM, Santora AC, Yates J, Meunier PJ. Alendronate increases bone strength by increasing the mean degree of mineralization of bone tissue in osteoporotic women. Bone. 2000;27(5):687–94.
31. Boivin G, Meunier PJ. Effects of bisphosphonates on matrix mineralization. J Musculoskelet Neuronal Interact. 2002;2(6):538–43.
32. Paschalis EP, DiCarlo E, Betts F, Sherman P, Mendelsohn R, Boskey AL. FTIR microspectroscopic analyses of human osteonal bone. Calcif Tissue Int. 1996;59(6):480–7.
33. Currey JD. Changes in the impact energy absorption of bone with age. J Biomech. 1979;12(6):459–69.
34. Paschalis EP, Betts F, DiCarlo E, Mendelsohn R, Boskey AL. FTIR microspectroscopic analyses of normal human cortical and trabecular bone. Calcif Tissue Int. 1997;61(6):480–6.
35. Grynpas M. Age and disease-related changes in the mineral of bone. Calcif Tissue Int. 1993;53 Suppl 1:S57–64.
36. Akkus O, Adar F, Schaffler MB. Age-related changes in physicochemical properties of mineral crystals are related to impaired mechanical function of cortical bone. Bone. 2004;34(3):443–53.
37. Paschalis EP, Verdelis K, Doty SB, Boskey AL, Mendelsohn R, Yamauchi M. Spectroscopic characterization of collagen cross-links in bone. J Bone Miner Res. 2001;16(10):1821–8.
38. Viguet-Carrin S, Garnero P, Delmas PD. The role of collagen in bone strength. Osteoporos Int. 2006;17(3):319–36.
39. Eyre DR, Dickson IR, Van Ness K. Collagen cross-linking in human bone and articular cartilage. Age-related changes in the content of mature hydroxypyridinium residues. Biochem J. 1988;252(2):495–500.
40. Wojtowicz A, Dziedzic-Goclawska A, Kaminski A, et al. Alteration of mineral crystallinity and collagen cross-linking of bones in osteopetrotic toothless (tl/tl) rats and their improvement after treatment with colony stimulating factor-1. Bone. 1997;20(2):127–32.
41. Saito M, Fujii K, Mori Y, Marumo K. Role of collagen enzymatic and glycation induced cross-links as a determinant of bone quality in spontaneously diabetic WBN/Kob rats. Osteoporos Int. 2006;17(10):1514–23.
42. Saito M, Marumo K. Collagen cross-links as a determinant of bone quality: a possible explanation for bone fragility in aging, osteoporosis, and diabetes mellitus. Osteoporos Int. 2010;21(2):195–214.
43. Akkus O, Polyakova-Akkus A, Adar F, Schaffler MB. Aging of microstructural compartments in human compact bone. J Bone Miner Res. 2003;18(6):1012–9.